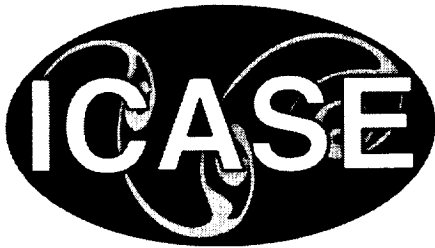NASA/CR-2002-211939
ICASE Report No. 2002-35

Quadratic Optimization in the Problems of Active Control of Sound

J. Loncaric
ICASE, Hampton, Virginia

S.V. Tsynkov
North Carolina State University, Raleigh, North Carolina and
Tel Aviv University, Tel Aviv, Israel

October 2002

The NASA STI Program Office ... in Profile

Since its founding, NASA has been dedicated to the advancement of aeronautics and space science. The NASA Scientific and Technical Information (STI) Program Office plays a key part in helping NASA maintain this important role.

The NASA STI Program Office is operated by Langley Research Center, the lead center for NASA's scientific and technical information. The NASA STI Program Office provides access to the NASA STI Database, the largest collection of aeronautical and space science STI in the world. The Program Office is also NASA's institutional mechanism for disseminating the results of its research and development activities. These results are published by NASA in the NASA STI Report Series, which includes the following report types:

- TECHNICAL PUBLICATION. Reports of completed research or a major significant phase of research that present the results of NASA programs and include extensive data or theoretical analysis. Includes compilations of significant scientific and technical data and information deemed to be of continuing reference value. NASA's counterpart of peer-reviewed formal professional papers, but having less stringent limitations on manuscript length and extent of graphic presentations.

- TECHNICAL MEMORANDUM. Scientific and technical findings that are preliminary or of specialized interest, e.g., quick release reports, working papers, and bibliographies that contain minimal annotation. Does not contain extensive analysis.

- CONTRACTOR REPORT. Scientific and technical findings by NASA-sponsored contractors and grantees.

- CONFERENCE PUBLICATIONS. Collected papers from scientific and technical conferences, symposia, seminars, or other meetings sponsored or cosponsored by NASA.

- SPECIAL PUBLICATION. Scientific, technical, or historical information from NASA programs, projects, and missions, often concerned with subjects having substantial public interest.

- TECHNICAL TRANSLATION. English-language translations of foreign scientific and technical material pertinent to NASA's mission.

Specialized services that complement the STI Program Office's diverse offerings include creating custom thesauri, building customized data bases, organizing and publishing research results ... even providing videos.

For more information about the NASA STI Program Office, see the following:

- Access the NASA STI Program Home Page at *http://www.sti.nasa.gov*

- Email your question via the Internet to help@sti.nasa.gov

- Fax your question to the NASA STI Help Desk at (301) 621-0134

- Telephone the NASA STI Help Desk at (301) 621-0390

- Write to:
  NASA STI Help Desk
  NASA Center for AeroSpace Information
  7121 Standard Drive
  Hanover, MD 21076-1320
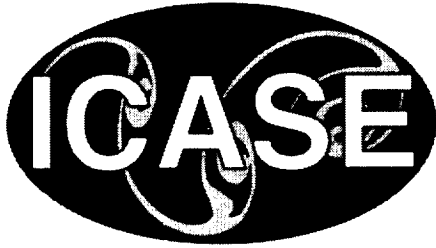
Quadratic Optimization in the Problems of Active Control of Sound

J. Loncaric
ICASE, Hampton, Virginia

S.V. Tsynkov
North Carolina State University, Raleigh, North Carolina and
Tel Aviv University, Tel Aviv, Israel

ICASE
NASA Langley Research Center
Hampton, Virginia

Operated by Universities Space Research Association

October 2002

QUADRATIC OPTIMIZATION IN THE PROBLEMS OF ACTIVE CONTROL OF SOUND*

J. LONČARIĆ[†] AND S. V. TSYNKOV[‡]

Abstract. We analyze the problem of suppressing the unwanted component of a time-harmonic acoustic field (noise) on a predetermined region of interest. The suppression is rendered by active means, i.e., by introducing the additional acoustic sources called controls that generate the appropriate anti-sound. Previously, we have obtained general solutions for active controls in both continuous and discrete formulations of the problem. We have also obtained optimal solutions that minimize the overall absolute acoustic source strength of active control sources. These optimal solutions happen to be particular layers of monopoles on the perimeter of the protected region. Mathematically, minimization of acoustic source strength is equivalent to minimization in the sense of L_1.

By contrast, in the current paper we formulate and study optimization problems that involve quadratic functions of merit. Specifically, we minimize the L_2 norm of the control sources, and we consider both the unconstrained and constrained minimization. The unconstrained L_2 minimization is certainly the easiest problem to address numerically. On the other hand, the constrained approach allows one to analyze sophisticated geometries. In a special case, we can compare our finite-difference optimal solutions to the continuous optimal solutions obtained previously using a semi-analytic technique. We also show that the optima obtained in the sense of L_2 differ drastically from those obtained in the sense of L_1.

Key words. noise cancellation, active control sources, volumetric and surface controls, general solution, monopoles and dipoles, radiation of waves, complex-valued quantities, L_2-minimization, overdetermined systems, least squares, unconstrained minimization, constrained minimization

Subject classification. Applied and Numerical Mathematics

1. Introduction. In the simplest possible formulation, the problem of active control of sound is posed as follows. Let $\Omega \subset \mathbb{R}^n$ be a given domain (bounded or unbounded), and Γ be its boundary: $\Gamma = \partial\Omega$, where the dimension of the space n is either 2 or 3. Both on Ω and on its complement $\Omega_1 = \mathbb{R}^n \backslash \overline{\Omega}$ we consider the time-harmonic acoustic field $u = u(x)$, $x \in \mathbb{R}^n$, governed by the non-homogeneous Helmholtz equation:

$$Lu \equiv \Delta u + k^2 u = f. \tag{1.1}$$

Equation (1.1) is subject to the Sommerfeld radiation boundary conditions at infinity, which for $n = 2$ are set as

$$u(x) = O\left(|x|^{-1/2}\right), \quad \frac{\partial u(x)}{\partial |x|} + iku(x) = o\left(|x|^{-1/2}\right), \quad \text{as } |x| \longrightarrow \infty, \tag{1.2a}$$

and for $n = 3$ as

$$u(x) = O\left(|x|^{-1}\right), \quad \frac{\partial u(x)}{\partial |x|} + iku(x) = o\left(|x|^{-1}\right) \quad \text{as } |x| \longrightarrow \infty. \tag{1.2b}$$

The Sommerfeld boundary conditions specify the direction of wave propagation, and distinguish between the incoming and outgoing waves at infinity by prescribing the outgoing direction only; they guarantee the unique solvability of the Helmholtz equation (1.1) for any compactly supported right-hand side $f = f(x)$. It is important to mention that as we are dealing hereafter with the traveling waves (radiation of sound toward infinity), all the resulting solutions will necessarily be complex-valued, otherwise it is impossible to account for the key phenomenon of variation of phase with the change of spatial location.

The source terms $f = f(x)$ in equation (1.1) can be located on both Ω and its complement $\Omega_1 = \mathbb{R}^n \backslash \overline{\Omega}$; to emphasize the distinction, we denote

$$f = f^+ + f^-, \quad \text{supp}\, f^+ \subset \Omega, \ \text{supp}\, f^- \subset \Omega_1. \tag{1.3}$$

Accordingly, the overall acoustic field $u = u(x)$ can be represented as a sum of the two components:

$$u = u^+ + u^-, \tag{1.4}$$

where u^+ is driven by the interior sources f^+, and u^- is driven by the exterior sources f^- w.r.t. Ω:

$$Lu^+ = f^+, \tag{1.5a}$$
$$Lu^- = f^-. \tag{1.5b}$$

Note, both $u^+ = u^+(x)$ and $u^- = u^-(x)$ are defined on the entire $\mathbb{R}^n$, the superscripts "+" and "−" refer to the sources that drive each of the field components rather than to the domains of these components. The setup described above is schematically shown in Figure 1.1 for the case of a bounded domain Ω.
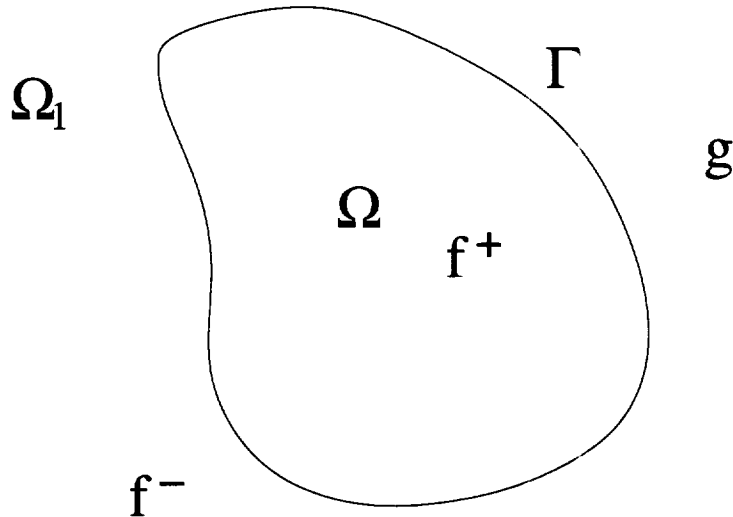
FIG. 1.1. *Geometric setup.*

Hereafter, we will call the component u^+ of (1.4), (1.5a) *sound*, or "friendly" part of the total acoustic field; the component u^- of (1.4), (1.5b) will accordingly be called *noise*, or "adverse" part of the total acoustic field. In the formulation that we are presenting, Ω will be a predetermined region of space to be protected from noise. This means that we would like to eliminate the noise component of $u(x)$ inside Ω, while leaving the sound component there unaltered. In the mathematical framework that we have adopted, the component u^- of the total acoustic field, i.e., the response to the adverse sources f^- [see (1.3), (1.4), (1.5)], will have to be canceled out on Ω, whereas the component u^+, i.e., the response to the friendly sources f^+, will have to be left unaffected on Ω. A physically more involved but conceptually easy to understand example that can be given to illustrate the foregoing idea, is that inside the passenger compartment of an aircraft we would like to eliminate the noise coming from the propulsion system located outside the fuselage, while not interfering with the ability of the passengers to listen to the inflight entertainment programs or simply converse. Another good example is found in medicine, where high levels of periodic noise are produced by resonance coils in magnetic resonance imaging (MRI) machines.

The concept of *active noise control* that we will be discussing implies that the component u^- is to be suppressed on Ω by introducing additional sources of sound $g = g(x)$ exterior with respect to Ω, supp $g \subset \Omega_1$, so that the total acoustic field $\tilde{u} = \tilde{u}(x)$ be now governed by the equation [cf. formulae (1.1), (1.3)]:

$$L\tilde{u} = f^+ + f^- + g, \tag{1.6}$$

and coincide with only the friendly component u^+ on the domain Ω:

$$\tilde{u}\big|_{x\in\Omega} = u^+\big|_{x\in\Omega}. \tag{1.7}$$

The new sources $g = g(x)$ of (1.6), see Figure 1.1, will hereafter be referred to as the *control sources* or simply *controls*. An obvious solution for these control sources is $g = -f^-$. This solution, however, is clearly sub-optimal because on one hand, it requires an explicit and detailed knowledge of the structure and location

of the sources f^-, which is, in fact, superfluous, see [4]. On the other hand, its implementation in many cases, like in the previously mentioned example with an airplane, may not be feasible. Fortunately, there are other solutions of the foregoing noise control problem (see Section 2, as well as our previous work [4] for detail), and some of them may be preferable from both the theoretical and practical standpoint.

To conclude the introduction, let us only mention that the area of active control of sound has a rich history of development, both as a chapter of theoretical acoustics, and in the perspective of many different applications. It is impossible to adequately overview this extensive area in the framework of a focused research publication. As such, we simply refer the reader to the monographs [1, 2, 7] that, among other things, contain a detailed survey of the literature. Potential applications for the active techniques of noise control range from the aircraft industry to manufacturing industry to ground and air transportation to the military to consumer products and other fields, including even such highly specialized and narrow areas as acoustic measurements in the wind tunnels. It is generally known that active techniques are more efficient for lower frequencies, and they are usually expected to complement passive strategies (sound insulation, barriers, etc.) that are more efficient for higher frequencies, because the rate of sound dissipation due to viscosity of the medium and heat transfer is proportional to the square of the frequency [3].

Let us also note that in the current paper we focus on the case of the standard constant-coefficient Helmholtz equation (1.1), which governs the acoustic field throughout the entire space $\mathbb{R}^n$. This allows us to make the forthcoming analysis most straightforward. However, one can as well consider other, more complex, cases that involve variable coefficients, different types of far-field behavior, discontinuities in the material properties, and maybe even nonlinearities in the governing equations over some regions. Approaches to obtaining solutions for active controls in these cases are based on the theory of generalized Calderon's potentials and boundary projections, and can be found in our previous paper [4] and in the monograph by Ryaben'kii [12, Part VIII].

The material in the rest of the paper is organized as follows. In Section 2, we introduce and discuss general solutions for controls in the continuous and discrete framework. Section 3 is devoted to the formulation and solution of the quadratic optimization problems for the control sources (unconstrained and constrained L_2 optimization). For reference purposes we also briefly mention our previous results on the optimization in the sense of L_1. Finally, Section 4 provides a summary and outlines a perspective for the future work.

2. General Solutions for Control Sources.

2.1. Continuous Formulation of the Problem.
A general solution for the volumetric continuous control sources $g = g(\boldsymbol{x})$ is given by the following formula ($\Omega_1 = \mathbb{R}^n \setminus \overline{\Omega}$):

$$g(\boldsymbol{x}) = -\boldsymbol{L}w\big|_{\boldsymbol{x} \in \Omega_1}, \tag{2.1}$$

where $w = w(\boldsymbol{x})$, $\boldsymbol{x} \in \Omega_1$, is a special auxiliary function-parameter that parameterizes the family of controls (2.1). The function $w(\boldsymbol{x})$ must satisfy the Sommerfeld boundary conditions (1.2a) or (1.2b) at infinity, and at the interface Γ, the function w and its normal derivative have to coincide with the corresponding quantities that pertain to the total acoustic field u given by formula (1.4):

$$w\big|_\Gamma = u\big|_\Gamma, \qquad \frac{\partial w}{\partial \boldsymbol{n}}\bigg|_\Gamma = \frac{\partial u}{\partial \boldsymbol{n}}\bigg|_\Gamma. \tag{2.2}$$

4

Other than that, the function $w(x)$ used in (2.1) is arbitrary, and consequently formula (2.1) defines a large family of control sources, which provides ample room for optimization. The justification for formula (2.1) as the general solution for controls can be found in [4]. In our recent paper [5] we also emphasize that the controls

$$g(x) = \int g(y)\delta(x - y)dy = g * \delta$$

given by (2.1) are *actually volumetric control sources of the monopole type* with regular density $g \in L_1^{(\text{loc})}(\mathbb{R}^n)$ [assuming that $w(x)$ was chosen sufficiently smooth to guarantee local absolute integrability of $g(x)$].

The control sources (2.1) possess several important properties. First of all, we see that to obtain these controls one needs no knowledge of the actual exterior sources of noise f^-. In other words, neither their location, nor structure, nor strength are required. All one needs to know is u and $\frac{\partial u}{\partial n}$ on the perimeter Γ of the protected region Ω. In a practical setting, $u|_\Gamma$ and $\frac{\partial u}{\partial n}|_\Gamma$ can be interpreted as measurable quantities that are supplied to the control system as the input data. Let us emphasize that the quantities to be measured refer to the overall acoustic field u rather than only to its unwanted component u^-, see formula (2.2). At the same time, the analysis of [4] shows that the application of the controls (2.1) will result in the cancellation of only the adverse noise u^- on the protected domain Ω, whereas the friendly sound field u^+ will be left unaffected. In other words, the controls (2.1) are insensitive to the interior sound u^+, whatever it might be, and are built so that to suppress only the exterior noise u^- on Ω. This capability is extremely important because in many applications the overall acoustic field always contains a component that needs to be suppressed along with the part that needs to be left intact. Let us also note that a more general analysis of [4] based on Calderon's potentials and boundary projections yields the same formula for controls (2.1), (2.2) for the cases that may involve variations in material properties and alternative types of the far-field behavior. Of course, the operator L will be a new variable-coefficient operator, and the function-parameter $w(x)$ will have to satisfy new far-field boundary conditions instead of the Sommerfeld boundary conditions.

Along with the volumetric controls (2.1), one can also consider *surface controls,* i.e., the control sources that are concentrated only on the interface Γ. A general solution for the surface controls is given by

$$g^{(\text{surf})} = - \left[\frac{\partial w}{\partial n} - \frac{\partial u}{\partial n}\right]_\Gamma \delta(\Gamma) - \frac{\partial}{\partial n}\left([w - u]_\Gamma \delta(\Gamma)\right), \tag{2.3}$$

where $w = w(x)$, as before, denotes the auxiliary function-parameter. In contradistinction to the previous case, now it has to satisfy the homogeneous Helmholtz equation on the complementary domain: $Lw = 0$ for $x \in \Omega_1$, and the Sommerfeld boundary condition (1.2a) or (1.2b) at infinity, but at the interface Γ it may be arbitrary, i.e., it does not have to meet boundary conditions (2.2). The corresponding discontinuities that are denoted by expressions in rectangular brackets in formula (2.3) drive the surface control sources. The first term on the right-hand side of (2.3) represents the density of a single-layer potential, which is a layer of monopoles on the interface Γ, and the second term on the right-hand side of (2.3) represents the density of a double-layer potential, which is a layer of dipoles on the interface Γ. A detailed justification of formula (2.3) as general solution for surface controls can be found in [15], see also [5]. The fundamental properties of the surface controls (2.3) are the same as those of the volumetric controls (2.1) — they are also insensitive to the interior sound $u^+(x)$, and do not require any knowledge of the actual sources of noise f^-.

In the family of surface controls (2.3) we identify two important particular cases. First, the cancellation of $u^-(x)$, $x \in \Omega$, can be achieved by using surface monopoles only, i.e., by employing only a single-layer

potential as the annihilating signal (anti-sound). To do that, we need to find $w(\boldsymbol{x})$, $\boldsymbol{x} \in \Omega_1$, such that there will be no discontinuity on Γ between $u(\boldsymbol{x})$ and $w(\boldsymbol{x})$, i.e., in the function itself, and the discontinuity may only "reside" in the normal derivative [see formula (2.3)]. This $w(\boldsymbol{x})$ will obviously be a solution of the following external Dirichlet problem:

$$
\begin{aligned}
\boldsymbol{L}w = 0, \quad \boldsymbol{x} \in \Omega_1, \\
w\big|_\Gamma = u\big|_\Gamma,
\end{aligned}
\tag{2.4}
$$

subject to the appropriate Sommerfeld boundary condition (1.2a) or (1.2b). Problem (2.4) is always uniquely solvable on $\Omega_1 = \mathbb{R}^n \backslash \overline{\Omega}$. Second, one can employ only the double-layer potential to cancel out $u^-(\boldsymbol{x})$, $\boldsymbol{x} \in \Omega$, i.e., use only surface dipoles as the control sources. In this case, the function $w(\boldsymbol{x})$, $\boldsymbol{x} \in \Omega_1$, has to be chosen such that the discontinuity on Γ be only in the function itself, i.e., between the actual values of $u(\boldsymbol{x})$ and $w(\boldsymbol{x})$, and not between the normal derivatives. This $w(\boldsymbol{x})$ should then solve the following external Neumann problem:

$$
\begin{aligned}
\boldsymbol{L}w = 0, \quad \boldsymbol{x} \in \Omega_1, \\
\frac{\partial w}{\partial \boldsymbol{n}}\bigg|_\Gamma = \frac{\partial u}{\partial \boldsymbol{n}}\bigg|_\Gamma,
\end{aligned}
\tag{2.5}
$$

again, subject to the appropriate Sommerfeld condition at infinity, (1.2a) or (1.2b); the latter guarantees the solvability of (2.5). We therefore see that surface control sources (2.3) are given by combinations of the monopole and dipole layers, with the two "extreme" cases corresponding to either only monopoles, see (2.4), or only dipoles, see (2.5).

Altogether, we have now introduced active controls of two different types on the surface, but only one type of the volumetric controls — monopoles, see formulae (2.1), (2.2). This is not accidental. Let us note that from the standpoint of physics and engineering, the monopole and dipole sources provide different types of excitation to the surrounding sound-conducting medium. A point monopole source can be interpreted as a vanishingly small pulsating sphere that radiates acoustic waves symmetrically in all directions, whereas a dipole source resembles a small oscillating membrane that has a particular directivity of radiation. Moreover, in the genuine time-dependent acoustic context one can show that monopole sources are those that alter the balance of mass in the system, they are scalar in nature and reside on the right-hand side of the continuity equation, whereas dipole sources alter the balance of force, they are vectors and reside on the right-hand side of the momentum equation, see our recent work [5] for detail. This distinction basically warrants a separate consideration of the monopole and dipole type sources as far as the point-wise or surface excitation may be concerned. As, however, has been shown in [5], in the framework of time-harmonic volumetric excitation (the case studied hereafter) a separate consideration of dipole fields appears superfluous. In fact, any volumetric distribution of dipoles can, under the assumption of sufficient regularity, be recast in the form of an equivalent volumetric distribution of monopoles. In so doing, the dipole sources enter the right-hand side of the Helmholtz equation (1.1) through a divergence operator, whereas monopoles enter this right-hand side directly (up to a multiplicative constant).[1] We refer the reader to our paper [5], as well as to the monograph [7], for further detail. In Section 3, we will study the volumetric monopole controls in the

---

[1] In the corresponding analysis, we interpret the field variable $u(\boldsymbol{x})$ as acoustic pressure, which is a common strategy in the literature.

context of L_2 optimization; for comparison, we also provide there the results of the L_1 optimization from [5] that involve both the volumetric and surface monopole control sources.

Let us also note that in practice it may often be convenient to use the so-called *artificial boundary conditions* (ABCs), see [14], as a part of the definition of the auxiliary function $w(x)$. Assume that there is a larger domain that fully contains Ω and require, in addition, that $Lw = 0$ outside this larger domain. This requirement is always met in the case of the surface controls (2.3); and in the case of the volumetric controls it implies that the resulting control sources will be compactly supported between Γ and the outer boundary of the aforementioned larger region, see formula (2.1). For many applications this is desirable. Moreover, from the standpoint of computing this is clearly the only feasible way to obtain a finite discretization (see Section 2.2). It is known that the homogeneous equation $Lw = 0$ outside a given region, along with the Sommerfeld boundary conditions at infinity, can be equivalently replaced by special ABCs at the boundary of this region. General approaches to building the ABCs for a variety of different formulations are discussed in the review paper [14]. For the specific case of a homogeneous Helmholtz equation outside a sphere of radius R in 3D, the ABCs were obtained in [5] using the separation of variables in spherical coordinates and mode selection that would guarantee that the boundary conditions at infinity are satisfied:

$$\left.\frac{d\hat{w}_{lm}}{d\rho}\right|_{\rho=R} = \frac{\frac{d}{d\rho}[\rho^{-1/2}H_{l+1/2}^{(2)}(k\rho)]}{\rho^{-1/2}H_{l+1/2}^{(2)}(k\rho)}\hat{w}_{lm}(\rho)\Big|_{\rho=R}. \tag{2.6}$$

In formula (2.6), ρ is the spherical radius, $\hat{w}_{lm}$ are the Fourier coefficients of $w(x)$ with respect to spherical functions Y_l^m, $l = 0, 1, 2, \ldots$, $m = 0, \pm 1, \ldots, \pm l$, and $H_{l+1/2}^{(2)}$ are Hankel's functions of the second kind; equalities (2.6) have to be enforced for all the appropriate l and m. Similarly, for the homogeneous Helmholtz equation outside a disk of radius R in 2D, the ABCs obtained in [5] read:

$$\left.\frac{d\hat{w}_l}{d\rho}\right|_{\rho=R} = \frac{\frac{d}{d\rho}H_l^{(2)}(k\rho)}{H_l^{(2)}(k\rho)}\hat{w}_l(\rho)\Big|_{\rho=R}, \tag{2.7}$$

where ρ is the polar radius, and $\hat{w}_l$ are the Fourier coefficients of $w(x)$ with respect to the complex exponents $e^{-il\theta}$, $l = 0, \pm 1, \pm 2, \ldots$; again, equalities (2.7) have to be enforced for all l.

2.2. Discrete Formulation of the Problem. The continuous analysis tools employed for obtaining the control sources of the previous Section 2.1 are obviously deficient from the standpoint of applications. Indeed, any practical design of a noise control system can only be composed of a finite number of elements (sensors for measuring the field and actuators for creating the appropriate excitation, i.e., anti-sound). Therefore, it is natural to discretize the problem on the grid and obtain the control sources in the discrete framework so that the locations of the sensors and actuators can be associated with the grid nodes. For details regarding the discrete formulation of the problem we refer the reader to the monograph [12, Part VIII], as well as to the papers [17, 18]; a brief account can also be found in [5, 15], and below we summarize the results. Note that our discrete analysis is not limited to any specific type of the grid. In particular, no adaptation or grid fitting to either the shape of the protected region Ω or that of the external artificial boundary, is generally required. However, for the purpose of illustrating the concepts discussed hereafter, we will use a two-dimensional example that involves a polar grid. The use of the polar grid greatly facilitates setting the discrete ABCs at the circular outer boundary of radius R. Moreover, the same two-dimensional polar example is analyzed later in Section 3 in the context of L_2 optimization.

Let us denote the aforementioned polar grid N; it spans both Ω and Ω_1. Of course, the grid does not extend all the way to infinity, it is rather truncated by the external artificial boundary in the shape of a large circle of radius R. This, in particular, implies that the discrete control sources that we obtain will always be compactly supported (see the discussion in the end of Section 2.1). Assume that the grid has J cells in the radial direction with the nodes $\rho_j = j\Delta\rho$, $j = 0, \ldots, J$, so that $\rho_0 = 0$ and $\rho_J = R$; and L cells in the circumferential direction with the nodes $\theta_s = s\Delta\theta$, $s = 0, \ldots, L$, so that $\theta_0 = 0$ and $\theta_L = 2\pi$. For simplicity, it is convenient to think that the grid sizes $\Delta\rho = R/J$ and $\Delta\theta = 2\pi/L$ are constant; in applications, however, the grid in the radial direction may be stretched.

Let now $u^{(h)}$ be a representation of the acoustic field on the grid, and $\boldsymbol{L}^{(h)}$ be a finite-difference approximation of the differential operator $\boldsymbol{L}$ of (1.1). To accurately define the approximation, we will need to introduce another grid M along with the previously defined N. On the grid M, we will consider the residuals of the operator $\boldsymbol{L}^{(h)}$, and subsequently the right-hand sides to the corresponding discrete inhomogeneous equation. We will use the notations n and m for the individual nodes of the grids N and M, respectively, and the notation N_m for the stencil of the discrete operator $\boldsymbol{L}^{(h)}$ centered at a given node $m \in \mathsf{M}$, so that

$$\boldsymbol{L}^{(h)} u^{(h)} \Big|_m = \sum_{n \in \mathsf{N}_m} a_{mn} u_n^{(h)}, \qquad (2.8)$$

where a_{nm} are the coefficients associated with particular nodes of the stencil. Generally, there are no limitations to the type of the discrete operator that one may use. We only require that the difference operator $\boldsymbol{L}^{(h)}$ of (2.8) approximate the differential operator $\boldsymbol{L}$ of (1.1) with the accuracy sufficient for a particular application. For the specific example that we are analyzing, we will consider a conventional second-order central-difference approximation, so that the grids N and M actually coincide: $n = (s,j)$ and $m = (s,j)$ (except that M is smaller, it does not contain the outermost row $\rho = \rho_J = R$), and formula (2.8) becomes:

$$\boldsymbol{L}^{(h)} u^{(h)} \Big|_{s,j} \equiv \frac{1}{\rho_j} \frac{1}{\Delta\rho} \left(\rho_{j+\frac{1}{2}} \frac{u_{s,j+1}^{(h)} - u_{s,j}^{(h)}}{\Delta\rho} - \rho_{j-\frac{1}{2}} \frac{u_{s,j}^{(h)} - u_{s,j-1}^{(h)}}{\Delta\rho} \right) + \frac{1}{\rho_j^2} \frac{u_{s+1,j}^{(h)} - 2u_{s,j}^{(h)} + u_{s-1,j}^{(h)}}{\Delta\theta^2} + k^2 u_{s,j}^{(h)}.$$

$$(2.9)$$

Next, we introduce the following subsets of the grids M and N, which will allow us to accurately distinguish between the interior and exterior domains, interior and exterior sources, and interior and exterior solutions on the discrete level:

$$\mathsf{M}^+ = \mathsf{M} \cap \Omega, \quad \mathsf{M}^- = \mathsf{M} \backslash \mathsf{M}^+ = \mathsf{M} \cap \Omega_1,$$

$$\mathsf{N}^+ = \bigcup_{m \in \mathsf{M}^+} \mathsf{N}_m, \quad \mathsf{N}^- = \bigcup_{m \in \mathsf{M}^-} \mathsf{N}_m, \qquad (2.10)$$

$$\gamma = \mathsf{N}^+ \cap \mathsf{N}^-, \quad \gamma^+ = \mathsf{N}^- \cap \Omega, \quad \gamma^- = \mathsf{N}^+ \cap \Omega_1.$$

We emphasize, that the grid M that pertains to the residuals of the finite-difference operator $\boldsymbol{L}^{(h)}$ is partitioned into M^+ and M^- directly, i.e., following the geometry of Ω and Ω_1. In contradistinction to that, the grid N is not partitioned directly, we rather consider the collection of all nodes of N swept by the stencil N_m when its center[2] belongs to Ω, and call this sub-grid N^+, see (2.10). Obviously, some of the nodes of

---

[2]These definitions require that the grid be sufficiently large to ensure that the sets M^+ and M^- are not empty; each must include at least one layer of nodes along the interface, as in formula (3.11), see Section 3.2.
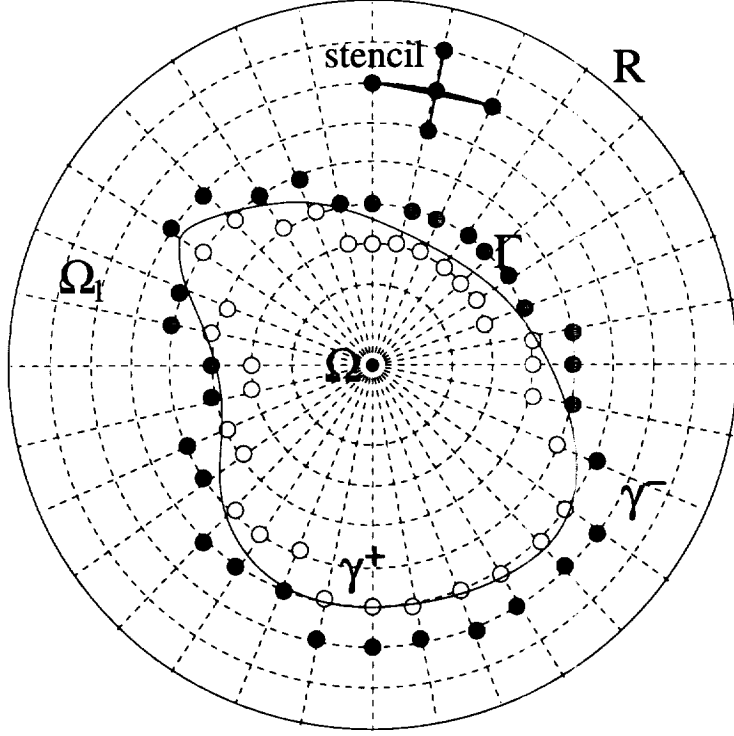
8

FIG. 2.1. *Schematic geometry of the domains, the stencil, and the grid boundary* $\gamma = \gamma^+ \cup \gamma^-$ *in polar coordinates: Hollow bullets denote* γ^+, *filled bullets denote* γ^-.

N^+ obtained by this approach happen to be outside Ω, i.e., in Ω_1, and these nodes are called γ^-. The sets N^- and γ^+ are defined similarly starting from M^-. The key idea is that whereas the grids M^+ and M^- do not overlap, the grids N^+ and N^- do overlap, and their overlap is denoted γ; obviously, $\gamma = \gamma^+ \cup \gamma^-$. The subset of grid nodes γ is called *the grid boundary*, it is a fringe of nodes that is located near the continuous boundary Γ and in some sense straddles it. The specific structure of γ clearly depends on the construction of the operator $L^{(h)}$ of (2.8) and the stencil N_m. For example, for the polar second-order Laplacian (2.9), the grid boundary γ will be a two-layer fringe of grid nodes located near Γ, as shown schematically in Figure 2.1. Further specifics on the construction of grid boundaries can be found in the monograph [12].

The discrete noise control problem is formulated similarly to the continuous one, see Section 1. Let $f_m^{(h)+}$, $m \in M^+$, and $f_m^{(h)-}$, $m \in M^-$, be the interior and exterior discrete acoustic sources, respectively. Let $u_n^{(h)+}$, $n \in N$, and $u_n^{(h)-}$, $n \in N$, be the corresponding solutions, i.e., $L^{(h)}u^{(h)+} = f^{(h)+}$ and $L^{(h)}u^{(h)-} = f^{(h)-}$. Using the same terminology as before, we will call $u^{(h)+}$ the discrete sound and $u^{(h)-}$ the discrete noise. The overall discrete acoustic field $u^{(h)}$ is the sum of its sound and noise components, $u^{(h)} = u^{(h)+} + u^{(h)-}$ on N, and obviously satisfies the equation $L^{(h)}u^{(h)} = f^{(h)} \equiv f^{(h)+} + f^{(h)-}$. The goal is to obtain the discrete control sources $g^{(h)} = g_m^{(h)}$ so that the solution $\tilde{u}^{(h)}$ of the equation $L^{(h)}\tilde{u}^{(h)} = f^{(h)+} + f^{(h)-} + g^{(h)}$ be equal to only the sound component $u^{(h)+}$ on the sub-grid N^+.

A general solution for the discrete control sources $g^{(h)} = g_m^{(h)}$ that eliminate the unwanted noise $u^{(h)-}$

on $\mathbb{N}^+$ is given by the following formula [cf. formula (2.1)]:

$$g_m^{(h)} = -L^{(h)} w^{(h)} \Big|_{m \in \mathsf{M}^-}, \tag{2.11}$$

where $w^{(h)} = w_n^{(h)}$, $n \in \mathbb{N}^-$, is a special auxiliary grid function-parameter that parameterizes the family of controls (2.11). The requirements that this function $w^{(h)}$ must satisfy are, again, rather "loose," and can be considered natural discrete counterparts of the corresponding requirements of the continuous function-parameter $w(\boldsymbol{x})$. Namely, at the grid boundary γ the function $w^{(h)}$ has to coincide with the overall acoustic field $u^{(h)}$ to be controlled:

$$w_n^{(h)} \Big|_{n \in \gamma} = u_n^{(h)} \Big|_{n \in \gamma}. \tag{2.12}$$

Notice that since, e.g., for the second-order discretizations the grid boundary γ contains two layers of nodes, γ^+ and γ^-, see Figure 2.1, then specifying the corresponding nodal values on γ is in some sense equivalent to specifying the function and its normal derivative on Γ in the continuous case, see (2.2).[3] We also note that for practical designs, the boundary data $u_n^{(h)}\big|_{n \in \gamma}$ shall be interpreted as measurable quantities that provide input for the control system. In other words, we can think of a microphone at every node of γ; these microphones measure the characteristics of the actual acoustic field and generate the input signal $u_n^{(h)}\big|_{n \in \gamma}$.

The other requirement of the function $w^{(h)}$, besides the interface boundary conditions (2.12), is that they must satisfy the appropriate discrete ABCs at the external artificial boundary $\rho = R$, see Figure 2.1. The role of the discrete ABCs is the same as that of the continuous ABCs — to provide a replacement for the Sommerfeld radiation boundary conditions. The discrete two-dimensional ABCs are obtained in [5] by using the direct and inverse discrete Fourier transforms, $l = -L/2 + 1, \ldots, L/2$, $s = 0, \ldots, L - 1$:

$$\hat{w}_l = \frac{1}{L} \sum_{s=0}^{L-1} w_s e^{-ils\Delta\theta}, \qquad w_s = \sum_{l=-L/2+1}^{L/2} \hat{w}_l e^{ils\Delta\theta}, \tag{2.13}$$

and essentially approximating boundary conditions (2.7) for $l = -L/2 + 1, \ldots, L/2$ with the second order of accuracy:

$$\frac{\hat{w}_{l,J} - \hat{w}_{l,J-1}}{\Delta\rho} - \beta_l \frac{\hat{w}_{l,J} + \hat{w}_{l,J-1}}{2} = 0, \quad \beta_l = \frac{\frac{d}{d\rho} H_{\alpha_l}^{(2)}(k\rho)}{H_{\alpha_l}^{(2)}(k\rho)} \Bigg|_{\rho=R}, \quad \alpha_l^2 = \frac{4}{\Delta\theta^2} \sin^2 \frac{l\Delta\theta}{2}. \tag{2.14}$$

Note, $-\alpha_l^2$ of (2.14) are eigenvalues of the circumferential component of the discrete Laplacian (2.9). Relations (2.14) for all $l = -L/2 + 1, \ldots, L/2$ can also be recast into the matrix form:

$$\boldsymbol{w}_{\cdot,J} = \boldsymbol{F}^{-1} \operatorname{diag} \left\{ -\left(\frac{1}{\Delta\rho} + \beta_l\right) \left(\frac{1}{\Delta\rho} - \beta_l\right)^{-1} \right\} \boldsymbol{F} \, \boldsymbol{w}_{\cdot,J-1} \equiv \boldsymbol{T} \, \boldsymbol{w}_{\cdot,J-1}, \tag{2.15}$$

where $\boldsymbol{F}$ and $\boldsymbol{F}^{-1}$ are matrices of the direct and inverse discrete Fourier transforms of (2.13), and $\boldsymbol{w}_{\cdot,J}$ and $\boldsymbol{w}_{\cdot,J-1}$ are L-dimensional vectors of components $w_{s,J}^{(h)}$ and $w_{s,J-1}^{(h)}$, respectively, $s = 0, 1, \ldots, L - 1$.

Other than the two aforementioned requirements, i.e., the interface conditions (2.12) and the ABCs (2.15), the function $w^{(h)}$ is arbitrary and as such, parameterizes a substantial variety of discrete control sources, see (2.11). The latter will provide the search space for optimization in Section 3.

---

[3]This statement can be given a rigorous formulation in terms of approximation, see [12] for detail.

It is also important to understand in what sense this discrete cancellation of noise models the continuous cancellation described in Section 2. This is basically the question of approximation of the continuous generalized Calderon's potentials by their discrete counterparts. To that effect, the theory of difference potentials, see [12], says that under certain natural conditions, the discrete anti-sound $v^{(h)} = v_n^{(h)}$, $n \in \mathbb{N}^+$, i.e., the solution to $L^{(h)} v^{(h)} = g^{(h)}$ with $g^{(h)}$ given by (2.11), approximates the continuous anti-sound $v = v(x)$, $x \in \Omega$, i.e., the solution to $Lv = g$ with g given by (2.1). The aforementioned natural conditions include first the consistency and stability of the finite-difference scheme for the Helmholtz equation. Consistency and stability will guarantee convergence as the grid size vanishes. In addition, the discrete boundary data $u_n^{(h)}\big|_{n \in \gamma}$ of (2.12) have to approximate the continuous boundary data $\left(u, \frac{\partial u}{\partial n}\right)\big|_\Gamma$ of (2.2) in the following sense. Once the continuous function u and its first-order normal derivative $\frac{\partial u}{\partial n}$ are known at the boundary Γ, normal derivatives of higher orders can be obtained via the differential equation itself, and the near-boundary values $u_n^{(h)}\big|_{n \in \gamma}$ can then be calculated using Taylor's expansion; the order of accuracy of the latter calculation with respect to the grid size h has to be at least as high as the order of accuracy of the interior scheme. In this case, the quality of approximation, i.e., the rate of convergence of the discrete potential to the continuous one with respect to h, will be the same as prescribed by the finite-difference scheme itself. For the central-difference operator (2.9), this rate is $O(h^2)$. In other words, when designing an active control system following the finite-difference approach, one can expect to have the actual noise cancellation in the same approximate sense as the solution of the finite-difference equation approximates the corresponding solution of the original differential equation. Note, in any particular practical setting we will need to require sufficient wave resolution on the grid, i.e., the waves of length $\lambda = 2\pi/k$, where k is the wavenumber in (1.1), will have to be well resolved by the specific discretization.

Finally, similarly to the continuous case we can identify some particular types of the discrete control sources. First, let us define another subset of the grid $\mathbb{M}$ (more precisely, of $\mathbb{M}^-$):

$$\mathbb{M}_{\text{int}}^- = \left\{ m \in \mathbb{M}^- \,\middle|\, \mathbb{N}_m \cap \gamma^+ = \emptyset \right\}.$$

Basically, $\mathbb{M}_{\text{int}}^-$ is the interior subset of $\mathbb{M}^-$, such that when the center of the stencil sweeps this subset, the stencil itself does not touch γ^+, see Figure 2.1. In other words, $\mathbb{M}_{\text{int}}^-$ is a subset of $\mathbb{M}^-$ such that

$$\bigcup_{m \in \mathbb{M}_{\text{int}}^-} \mathbb{N}_m = \mathbb{N}^- \setminus \gamma^+.$$

Next, we introduce the auxiliary function $w^{(h)} = w_n^{(h)}$, $n \in \mathbb{N}^-$, for (2.11) as follows:

$$w_n^{(h)}\big|_{n \in \gamma^+} = u_n^{(h)}\big|_{n \in \gamma^+}, \tag{2.16a}$$

and

$$w_n^{(h)}\big|_{n \in \gamma^-} = u_n^{(h)}\big|_{n \in \gamma^-},$$
$$L^{(h)} w^{(h)} = 0 \quad \text{on} \quad \mathbb{M}_{\text{int}}^-. \tag{2.16b}$$

As before, we also assume that $w^{(h)}$ satisfies the discrete ABCs (2.15). Definition (2.16a) means that on the interior part of the grid boundary γ^+ we simply set $w^{(h)}$ equal to the given $u^{(h)}$: $w_n^{(h)}\big|_{n \in \gamma^+} = u_n^{(h)}\big|_{n \in \gamma^+}$. Definition (2.16b) is actually a discrete exterior boundary-value problem of the Dirichlet type. Indeed,

everywhere on and "outside" the exterior part of the grid boundary γ^-, i.e., on $N^- \backslash \gamma^+$, the grid function $w^{(h)}$ is obtained as a solution of the homogeneous equation $L^{(h)} w^{(h)} = 0$ (enforced at the nodes M_{int}^-) supplemented by the boundary data on γ^-: $w_n^{(h)}\big|_{n \in \gamma^-} = u_n^{(h)}\big|_{n \in \gamma^-}$, which is specified for the unknown function $w^{(h)}$ itself. Note, relation (2.16a) and the first relation (2.16b) together are obviously equivalent to (2.12). Therefore, the function $w^{(h)}$ defined via (2.16a), (2.16b) falls into the general class of $w^{(h)}$'s used for obtaining the discrete control sources (2.11).

Problem (2.16b) can clearly be considered a finite-difference counterpart to the continuous Dirichlet problem (2.4). Therefore, its is natural to call the control sources $g^{(h)} \equiv g_{monopole}^{(h,surf)}$ obtained by formulae (2.11), (2.16a), (2.16b) *the discrete surface monopoles*. Indeed, because of the definition of $w^{(h)}$ given by (2.16a) and (2.16b), these $g_{monopole}^{(h,surf)}$ may, generally speaking, differ from zero only on the grid set $M^- \backslash M_{int}^-$, which is a single "curvilinear" layer of nodes of grid M that follows the geometry of Γ. Accordingly, the output of these controls can be called the discrete single-layer potential. The discrete surface monopoles and discrete single-layer potential were first introduced and analyzed in our recent paper [15]. As shown in [5], the controls of this particular type play a key role in the context of L_1 optimization, see also Section 3.1. Let us emphasize that unlike the continuous surface controls (2.3), which belong to a different class of functions rather than the volumetric sources (2.1) (singular δ-type distributions vs. regular locally integrable functions), the foregoing discrete surface monopoles belong to the same original class of discrete control sources (2.11). Let us also note that besides the discrete surface monopoles and the corresponding single-layer potential, one can also define the discrete surface dipoles and, accordingly, the double-layer potential, see [15] for detail.

3. Optimization of the Control Sources. Once the general solution for controls is available, in either continuous (2.1) or discrete (2.11) formulation, the next step is to decide what particular element of this large family of functions will be optimal for a specific setting. There is a multitude of possible criteria for optimality that one can use. In many practical problems the cancellation of noise is only approximate and as such, the key criterion for optimization (or sometimes, the key constraint) is the quality of this cancellation, i.e., the extent of noise reduction. In contradistinction to that, in this paper we are considering ideal, or exact, cancellation, i.e., every particular control field from either the continuous (2.1) or discrete (2.11) family completely eliminates the unwanted noise on the domain of interest. Consequently, the criteria for optimality of the controls that we can employ will not include the level of the residual noise as a part of the corresponding function of merit, and should rather depend only on the control sources themselves. At a later stage of the work we plan to look into the issues of approximate, rather than identical, noise cancellation, for the reason of further reducing the costs. In this case, optimal solutions that still guarantee the exact cancellation are likely to provide good initial guesses for subsequent optimization in the approximate framework.

As indicated previously, in the current paper we focus primarily on the *quadratic optimization criteria*. We have looked into the most natural criterion of this type, namely, the L_2 norm of the control sources $g(x)$ of (2.1) or $g_m^{(h)}$ of (2.11), see Section 3.2. Clearly, this cost function depends only on the controls themselves. The advantage of minimizing the controls in the sense of L_2:

$$\|g\|_2 \equiv \sqrt{\int_{supp\, g} |g(x)|^2 dx} \longrightarrow \min \tag{3.1}$$

is that *the minimum can be easily computed*, see Section 3.2. The search space for minimization (3.1) includes

all the appropriate auxiliary functions $w(x)$, on which $g(x)$ depends. The disadvantage of using this criterion is that the quantity $\|g\|_2$ does not have a clear physical interpretation. Nonetheless, motivated primarily by the ease of the numerical approach to minimization, we do provide in Section 3.2 a comprehensive set of computed optimal solutions for active controls in the sense of the least squares (i.e., L_2). We also compare these discrete results with the "semi-analytic" L_2-optimal solutions obtained for simple circular shapes using the spectral methodology developed in our previous paper [4].

Note, an alternative to minimization in the sense of L_2 (3.1) may be minimization in the sense of L_1:

$$\|g\|_1 \equiv \int\limits_{\text{supp}\, g} |g(x)| dx \longrightarrow \min.$$

We have thoroughly studied this problem in our recent paper [5]. In particular, we have shown that the L_1 minimization is equivalent to minimizing *the overall absolute acoustic source strength*, see [6, 7], of the control sources $g(x)$. This clear physical interpretation constitutes an advantage of using the L_1 norm of the control sources as a cost function for optimization (besides that it also depends only on the control sources $g(x)$ themselves). On the other hand, the corresponding optimization problem has proven difficult to solve numerically, see [5]. We briefly describe the L_1 results of [5] in Section 3.1 for the purpose of comparison.

In the discrete framework, the L_2 minimization problem for the control sources can be formulated as follows:

$$\left\|g^{(h)}\right\|_2 \equiv \sqrt{\sum_{m \in \mathsf{M}^-} V_m |g_m^{(h)}|^2} \longrightarrow \min,$$

and the L_1 minimization problem can be formulated as follows:

$$\left\|g^{(h)}\right\|_1 \equiv \sum_{m \in \mathsf{M}^-} V_m |g_m^{(h)}| \longrightarrow \min,$$

where V_m accounts for the cell area and again, the search space includes all the appropriate auxiliary grid functions $w^{(h)}$, through which $g^{(h)}$ is defined, see formula (2.11).

Either of the two foregoing discrete minimization problems can also be rewritten using matrices. The finite-difference operator $L^{(h)}$ can obviously be interpreted as a matrix with N columns and M rows, where N is the number of nodes $n \equiv (s, j)$ of the grid N^- such that $\rho_j \leq R$, i.e., $j \leq J$, and M is the number of nodes $m \equiv (s, j)$ of the grid M^- such that $\rho_j < R$, i.e., $j \leq J - 1$. Let w be the vector of N components $w_n^{(h)} \equiv w_{s,j}^{(h)}$, $n \in \mathsf{N}^-$ and $j \leq J$, arranged so that

$$w = [w_\gamma, w_0, w_{\cdot, J-1}, w_{\cdot, J}]^T, \tag{3.2}$$

where w_γ contains $w_n^{(h)}$ for which $n \in \gamma$, $w_{\cdot, J}$ and $w_{\cdot, J-1}$ correspond to the outermost and second to last circles of the polar grid, respectively, as in formula (2.15), and w_0 contains all the remaining components of w "in-between" γ and the outer boundary. In accordance with (3.2), the matrix $L^{(h)}$ can be decomposed into four sub-matrices:

$$L^{(h)} = [A, B, C, D] \tag{3.3}$$

that all have the same number of rows M, A has as many columns as there are nodes in γ (we denote this number $|\gamma|$), C and D each has L columns, and B has $N - |\gamma| - 2L$ columns.

Using formulae (3.2) and (3.3) and introducing a generic notation $\| \cdot \|$ for either $\| \cdot \|_1$ or $\| \cdot \|_2$, we have:

$$\| V(A w_\gamma + B w_0 + C w_{.,J-1} + D w_{.,J}) \| \longrightarrow \min, \tag{3.4}$$

where V is an $M \times M$ diagonal matrix with the entries given by the corresponding cell areas V_m. The vector w in the optimization formulation (3.4) is, in fact, subject to a number of equality-type constraints that come from the interface conditions (2.12) and ABCs (2.15). More precisely, the first sub-vector w_γ in (3.2) is known and fixed because of (2.12) and we can rewrite (2.12) as $w_\gamma = u_\gamma$, where u_γ is given. The last sub-vector $w_{.,J}$ in (3.2) is a function of $w_{.,J-1}$ according to (2.15). Therefore, we can conclude that only w_0 and $w_{.,J-1}$ contain free variables that provide the search space for optimization, and as such rewrite (3.4) as

$$\min_{w_0, w_{.,J-1}} \| V(B w_0 + (C + DT) w_{.,J-1} + A w_\gamma) \| \equiv \min_z \| E z - f \|, \tag{3.5}$$

where $E = V[B, C + DT]$ is an $M \times (N - |\gamma| - L)$ given matrix, $z = [w_0, w_{.,J-1}]^T$ is an $(N - |\gamma| - L)$-dimensional vector of unknowns, and $f = -VA w_\gamma$ is an M-dimensional known vector of the right-hand side. Minimization problem (3.5) is, in fact, a problem of finding a weak solution of an overdetermined complex linear system $E z = f$. Note, the quantities involved are complex because we are dealing with the traveling waves in the framework of the Helmholtz equation (see Section 1).

3.1. Results of Optimization in the Sense of L_1. To provide a "reference point" for comparison, we outline here the findings of our recent work [5]. Because of the complex-valued quantities involved, the computation of the weak solution of problem (3.5) in the sense of L_1 reduces to solving a non-linear and non-smooth problem of constrained optimization over a large set of cones. This problem presents a substantial challenge even for the most sophisticated state-of-the-art approaches to numerical optimization, namely, those based on interior point methods [8, 16]. The difficulties are further exacerbated by the large dimension of the grid, because on one hand, the number of conical constraints that one obtains when solving (3.5) in the sense of L_1 is the same as the number of nodes in the grid M, which can be quite large even in two space dimensions, and on the other hand, the typical maximum number of constraints that the aforementioned state-of-the art methods can handle is only on the order of hundreds.

In spite of the difficulties, we have been able to compute several two-dimensional solutions for simple test cases. Our best results were obtained with the software package SeDuMi by J. F. Sturm.[4] This is a numerical algorithm for optimization over cones [13], it employs the ideas of interior-point methods, and the self-dual embedding technique of [19], see also [9]. The algorithm allows for complex-valued entries, which is very important in our framework, and also for quasi-convex quadratic and positive semi-definite constraints.

All numerical experiments that we have conducted, see [5], indicate a very consistent behavior of the L_1 optimal solution for the control sources. It happens to be the discrete layer of surface monopoles $g_{\mathrm{monopole}}^{(h,\,\mathrm{surf})}$ described in the concluding part of Section 2. Recall, this solution is obtained by applying formula (2.11) to the auxiliary function $w^{(h)}$ defined by (2.16a), (2.16b). Figure 3.1 reproduces the results of one particular computation from [5]; the protected region Ω for this case was a unit disk, and the grid dimension was chosen 32×7 (see Section 3.2.1 for the actual grid definition).

Motivated by the consistent observations of the L_1 optimal solution being the same as surface monopoles $g_{\mathrm{monopole}}^{(h,\,\mathrm{surf})}$, we have also been able to prove in [5] that surface monopoles indeed provide a global minimum for

---

[4]http://fewcal.kub.nl/sturm/software/sedumi.html
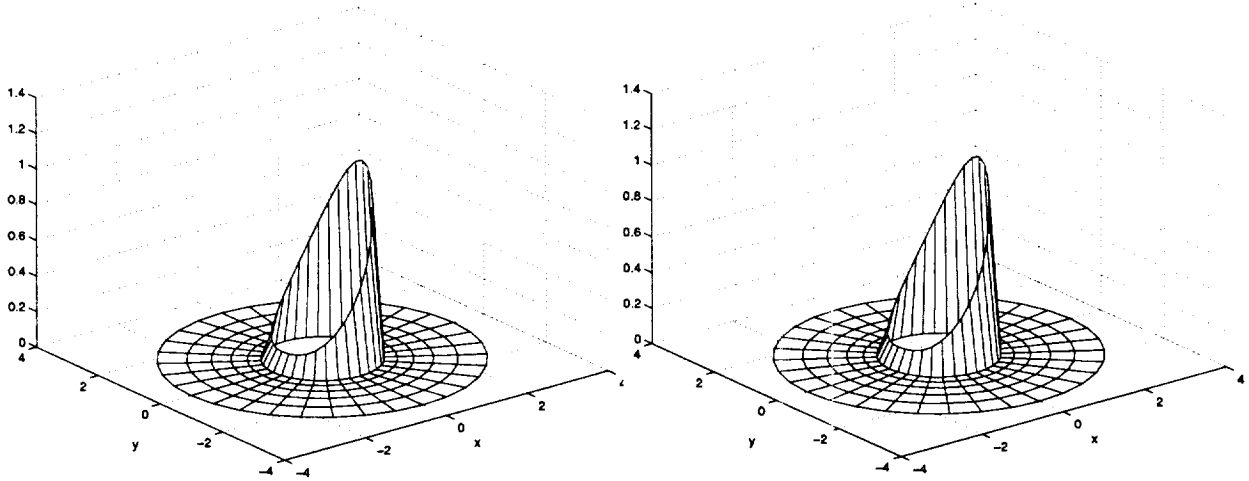
(a) L_1 optimal solution

(b) Surface monopoles $g_{\text{monopole}}^{(h,\text{surf})}$

FIG. 3.1. *Magnitude of the control sources for* $\Omega = \{x \in \mathbb{R}^2 \big| |x| < 1\}$, $k = 0.5$, $f^- = \delta(x - x_1)$, $x_1 = (5,0)$.

the control sources in the sense of L_1 for both the discrete and continuous formulation of the problem. The proof of [5], however, covers only the one-dimensional case. Even though we have not yet been able to prove a similar result for the general multi-dimensional case, we still believe that it is true, because a combination of the two-dimensional numerical evidence and a one-dimensional accurate proof cannot, in our opinion, be a mere coincidence. Therefore, we formulated this result in [5] in the form of a conjecture that we reproduce below. Let us remind, that according to (2.3) the continuous surface monopole controls are given by

$$g_{\text{monopole}}^{(\text{surf})}(x) = - \left[\frac{\partial w}{\partial n} - \frac{\partial u}{\partial n} \right]_\Gamma \delta(\Gamma) \equiv \nu(x)\Big|_{x \in \Gamma} \cdot \delta(\Gamma), \tag{3.6}$$

where $w(x)$ is a solution to the exterior Dirichlet problem (2.4). Then, we have

CONJECTURE 3.1. *Let a complex-valued function* $w = w(x)$ *be defined on* $\Omega_1 = \mathbb{R}^n \setminus \overline{\Omega}$, *and let it be sufficiently smooth so that the operator* L *of (1.1) can be applied to* $w(x)$ *on its entire domain in the classical sense, and the result* Lw *be locally absolutely integrable. Let, in addition. $w(x)$ satisfy the interface conditions (2.2), where* $u = u(x)$ *is a given field to be controlled, and the appropriate Sommerfeld radiation boundary conditions at infinity, (1.2a) or (1.2b). Then, the greatest lower bound for the* L_1 *norms of all the control sources* $g(x)$ *obtained with such auxiliary functions* $w(x)$ *using formula (2.1), is given by the* L_1 *norm on* Γ *of the magnitude of surface monopoles (3.6):*

$$\inf_{w(x)} \int_{\Omega_1} |g(x)| dx = \int_\Gamma |\nu(x)| ds. \tag{3.7}$$

Formula (3.7) can obviously be rewritten as

$$\inf_{w(x)} \|g(x)\|_{1,\Omega_1} = \|\nu\|_{1,\Gamma}. \tag{3.8}$$

As has been mentioned, the discrete prototype of formula (3.8) that reads as follows

$$\min_{w^{(h)}} \left\|g^{(h)}\right\|_{1,\text{M}^-} = \left\|g_{\text{monopole}}^{(h,\text{surf})}\right\|_{1,\gamma^-} \Delta\rho$$

15

was conjectured in [5] on the basis of the two-dimensional experimental observations. We emphasize that in the discrete case the L_1-optimal solution $g_{\text{monopole}}^{(\text{h,surf})}$ belongs to the same class of functions as all the discrete volumetric controls $g_m^{(h)}$ of (2.11), whereas in the continuous case the optimum on the class of volumetric controls $g(x)$ of (2.1) actually takes us out of this class to the singular layer (3.6) on the interface Γ.

3.2. Discrete Optimization in the Sense of L_2. The L_2 minimization problem for the volumetric control sources is solved hereafter completely on the discrete level. In other words, for every particular setup we are finding the minimum (3.5) or, equivalently, computing a weak solution of the overdetermined system of linear equations $Ez = f$, in the sense of the least squares. The resulting optima do not reduce to any clearly identifiable special cases, like the layer of surface monopoles that appeared in the previously analyzed context of L_1. They are not assigned any particular physical meaning either, we present them below in order to demonstrate that the L_2 optima are distinctly different from the L_1 optima obtained in [5], and that they can be easily computed numerically, including some cases that involve rather sophisticated geometry. In the simple case when the protected region Ω is a disk, we also conduct a grid convergence study in order to validate the results of the discrete L_2 minimization against the analytic reference solutions computed with high accuracy using the spectral methodology that was first proposed in [4].

PROPOSITION 3.1. *The matrix $E = V[B, C + DT]$, see formulae (3.3), (3.5), has full column rank.*

Proof. The justification of Proposition 3.1 will be based on a natural solvability assumption for the system of finite-difference equations that we are using. First, let us introduce more detailed partitions of w and $L^{(h)}$ instead of (3.2) and (3.3), respectively:

$$w = [w_{\gamma+}, w_{\gamma-}, w_0, w_{\cdot, J-1}, w_{\cdot, J}]^T,$$
$$L^{(h)} = [A^+, A^-, B, C, D]. \tag{3.9}$$

The matrices A^+ and A^- of (3.9) together give A of (3.3); $w_{\gamma+}$ and A^+ correspond to the innermost "half" of the grid boundary γ^+, and $w_{\gamma-}$ and A^- correspond to the outermost "half" of the grid boundary γ^- (see formula (2.10) and Figure 2.1). Next, consider an auxiliary exterior Dirichlet problem for the finite-difference equation $L^{(h)}u^{(h)} = 0$ [see formula (2.9)] with the boundary data specified at γ^+. As before, the problem is supposed to be truncated at the external artificial boundary $\rho = \rho_J$ by means of the ABC (2.15). This problem is a discrete counterpart of the continuous exterior Dirichlet problem for the Helmholtz equation with the boundary data given at Γ and ABCs (2.7) specified at $\rho = R$. The continuous problem is uniquely solvable because it is equivalent to the genuine infinite-domain exterior Dirichlet problem with the Sommerfeld boundary conditions (1.2b) set at infinity. Even though we do not prove it, it is certainly reasonable to assume that the corresponding discrete problem based on a standard central-difference scheme (2.9) and ABC (2.15) is uniquely solvable as well.[5] The latter assumption implies that the square $M \times M$ matrix $[A^-, B, C + DT]$, see formula (3.9), is non-singular. Consequently, the matrix $G = V[A^-, B, C + DT]$ is also non-singular, because V is an $M \times M$ diagonal matrix with non-zero diagonal entries V_m. Finally, we notice that the matrix $E = V[B, C + DT]$, see formulae (3.2) and (3.3), is obtained by removing the first $|\gamma^-|$ columns of the previous matrix G. Therefore, the columns of E are linearly independent. $\square$

---

[5] A proof of this fact would involve showing that relations (2.14) are "sufficiently close" to guaranteeing the precise mode selection in the discrete case so that to avoid the resonances. This task is beyond the scope of the current paper. A comprehensive study of solvability and well-posedness of one-dimensional discrete boundary value problems can be found in [11].

An obvious key implication of Proposition 3.1 is that the minimization problem (3.4), or equivalently (3.5), can be solved in the sense of L_2 (least squares) using a standard QR-based approach, i.e., without employing the Moore-Penrose type arguments. We use the MATLAB function LSQLIN for solving the least squares minimization problems hereafter. This function also allows one to do constrained minimization, the capability that we employ in Section 3.2.2.

3.2.1. Comparison with the Analytic Solution. In our previous work [4] we have developed a methodology of spectral type that allowed us to construct the continuous L_2-optimal volumetric controls for a particular geometry, namely, controls supported on annular domains. We employed the separation of variables and expressed the exact optimum as an infinite Fourier series in the circumferential direction whose coefficients were certain combinations of Bessel functions, see [4, formula(5.21)]. This series obviously had to be truncated at a certain maximum number of harmonics for the purpose of numerical evaluation. On smooth solutions, this method obviously provides for a spectral convergence. For the current purpose of validating the finite-difference algorithm we will use the spectral solution of [4] as a reference solution in the grid convergence tests.

Let the protected region be a disk of radius r centered at the origin: $\Omega = \{(\rho, \theta) | \rho < r\}$, and let the controls be supported on the annulus $\Omega_1 = \{(\rho, \theta) | r \leq \rho \leq R\}$. We introduce a simple conformal polar grid, which is uniform in the circumferential direction and stretched in the radial direction so that the cell aspect ratio is equal to one:

$$
\begin{aligned}
\mathbb{M} &= \{(\rho_j, \theta_s) | \, \rho_j = e^{j\Delta\theta}, j = 0, \ldots, J - 1; \, \theta_s = s\Delta\theta, s = 0, \ldots, L - 1; \, \Delta\theta = 2\pi/L\}, \\
\mathbb{N} &= \{(\rho_j, \theta_s) | \, \rho_j = e^{j\Delta\theta}, j = -1, 0, \ldots, J; \, \theta_s = s\Delta\theta, s = 0, \ldots, L - 1; \, \Delta\theta = 2\pi/L\}.
\end{aligned}
\tag{3.10}
$$

We, of course, assume that the area covered by the grid $\mathbb{N}$ of (3.10) is larger than Ω_1, i.e., $\rho_{-1} < r < R < \rho_J$. The Helmholtz operator can be easily approximated on the grid (3.10) with the second order of accuracy using the same five-node stencil as shown in Figure 2.1. This approximation involves only minor changes compared to the approximation (2.9) that works on uniform grids, and we refer the reader to our paper [10] for detail. The discrete ABCs in the form (2.14) or (2.15) do not change, except that $\Delta\rho$ needs to be replaced by $\Delta\rho_J = \rho_J - \rho_{J-1}$. Let us also note that we do not consider the grid (3.10) inside the domain Ω because we introduce it only for the purpose of obtaining the control sources on Ω_1. If, however, we were to actually compute the output of the controls inside the protected region, we would have had to extend the grid (3.10) all the way into Ω, which can obviously be done using a variety of strategies. As indicated by the previous analysis [4, 12, 17, 18], as long as the discrete controls are constructed according to formulae (2.11), (2.12), their output on the grid inside Ω will identically cancel out the unwanted acoustic component $u^{(h)-}$, see Section 2.2. In all the cases that we analyze hereafter, we have $\rho_{-1} < r \leq \rho_0$, so that according to (2.10) the grid subsets are defined as

$$
\begin{aligned}
\mathbb{M}^+ &= \{(\rho_j, \theta_s) | j = -1\}, \quad \mathbb{M}^- = \{(\rho_j, \theta_s) | 0 \leq j \leq J - 1\}, \\
\mathbb{N}^+ &= \{(\rho_j, \theta_s) | j = -1, 0\}, \quad \mathbb{N}^- = \{(\rho_j, \theta_s) | -1 \leq j \leq J\}, \\
\gamma &= \{(\rho_j, \theta_s) | j = -1, 0\}, \quad \gamma^+ = \{(\rho_j, \theta_s) | j = -1\}, \quad \gamma^- = \{(\rho_j, \theta_s) | j = 0\},
\end{aligned}
\tag{3.11}
$$

where always $s = 0, \ldots, L - 1$. In so doing, the dimension of the matrix $\boldsymbol{L}^{(h)}$, see (3.3), is $M \times N \equiv (L \cdot J) \times (L \cdot (J + 2))$, the dimension of $\boldsymbol{A}$, which corresponds to the variables on γ, is $M \times 2 \cdot L \equiv (L \cdot J) \times 2 \cdot L$,

the dimension of B is $M \times (N - 4L) \equiv (L \cdot J) \times (L \cdot (J - 2))$, and the dimension of either C or D is $M \times L \equiv (L \cdot J) \times L$.

We test the convergence of the discrete scheme for the wavenumber $k = 1.0$ and the excitation (i.e., the acoustic field $u^{(h)}$ that drives the control system) taken in the analytic form of a shifted fundamental solution of the Helmholtz operator, as if it were generated by the point source $f^- = \delta(\boldsymbol{x} - \boldsymbol{x}_1)$, where $\boldsymbol{x}_1 = (\rho \cos \theta, \rho \sin \theta) = (5, 0)$. We reemphasize that our approach does not require the explicit knowledge of the exterior sources of noise. We only need this function $u^{(h)}$ as a sample field to be used as given data in formula (2.12).

We employ a sequence of seven grids: $L \times J = 32 \times 3,\ 48 \times 4,\ 64 \times 5,\ 96 \times 7,\ 128 \times 9,\ 192 \times 13$, and 256×17, so that for all the grids the value of ρ_{J-1} is the same: $\rho_{J-1} = \text{const} \approx 1.481$; according to (3.10) we also have $\rho_0 = 1$. For the first series of convergence tests we assume that the boundaries $\rho = r$ and $\rho = R$ of the region Ω_1, on which the continuous controls are to be supported, are located exactly at the conformal midpoint of the first and last cell of the radial grid $\mathbb{N}$ of (3.10), respectively, i.e., $r = e^{-1/2\Delta\theta}$ and $R = e^{(J-1/2)\Delta\theta}$. The results of these tests are summarized in Table 3.1, which shows the L_2 norm of the relative error between the optimal continuous and discrete controls: $\arg\left[\min_{w(\boldsymbol{x})} \|g_{\text{spect}}(\boldsymbol{x})\|_2\right]$ and $\arg\left[\min_{w^{(h)}} \|g^{(h)}\|_2^{(h)}\right]$.

TABLE 3.1

Grid convergence for: $k = 1$, $f^- = \delta(\boldsymbol{x} - \boldsymbol{x}_1)$, $\boldsymbol{x}_1 = (5, 0)$, $r = e^{-1/2\Delta\theta}$, $R = e^{(J-1/2)\Delta\theta}$.

Grid	32×3	48×4	64×5	96×7	128×9	192×13	256×17
$\|\text{Error}\|_2$	0.013722	0.0061417	0.0034693	0.0015491	0.00087349	0.00038921	0.00021922

The data in Table 3.1 clearly indicate the second order of grid convergence for the discrete optimal controls $g^{(h)}$. It is important to emphasize, though, that the geometry of Ω_1 was chosen grid dependent (boundaries $\rho = r$ and $\rho = R$ were located at cell midpoints), which essentially means that for each subsequent grid in Table 3.1 the optimum was computed on a somewhat different (smaller) domain. It is quite obvious that in general the optimal solution will depend on the region on which the optimization is performed, and we cannot expect the optimum computed on a subdomain to coincide with the corresponding fragment of the optimum computed on the entire domain. However, the decrease of the error with the refinement of the grid observed in Table 3.1 shall still be interpreted as convergence. Indeed, had we continued refining the grid further, all the domains $\Omega_1 = \{r \leq \rho \leq R\}$ themselves would converge to one and the same annular region with the inner radius $r = \rho_0 = 1$ (Ω is a unit disk) and outer radius $R = \rho_{J-1}$, which was chosen grid independent.

On the other hand, the quadratic rate of convergence suggested by Table 3.1 appears a rather fragile phenomenon determined by the particular choice of the geometry. For other choices, the convergence may be slower. In Table 3.2, we present the results that correspond to the same inner boundary $r = e^{-1/2\Delta\theta}$, and the outer boundary located at either one quarter point or three quarters point of the outermost cell: $R = e^{(J-3/4)\Delta\theta}$ or $R = e^{(J-1/4)\Delta\theta}$. One can easily see that the convergence in Table 3.2 is only linear.

At the moment, we do not have a detailed explanation of the grid convergence properties for $g^{(h)}$ that we have observed, see Tables 3.1 and 3.2. It is important to realize, however, that what we evaluate is, in fact, convergence of the residual rather than that of the solution. Indeed, the solution of the optimization problem (3.4) or (3.5) per se is a particular grid function $w^{(h)}$ that delivers minimum to the selected function

TABLE 3.2

Relative L_2 error for: $k = 1$, $f^- = \delta(x - x_1)$, $x_1 = (5, 0)$, $r = e^{-1/2\Delta\theta}$, $R = e^{(J-3/4)\Delta\theta}$ and $R = e^{(J-1/4)\Delta\theta}$.

Grid	32×3	48×4	64×5	96×7	128×9	192×13	256×17
$J - 3/4$	0.10283	0.074135	0.058274	0.040958	0.031618	0.021733	0.016562
$J - 1/4$	0.096894	0.071804	0.057069	0.040476	0.031362	0.021627	0.016504

of merit, namely, the L_2 norm of the residual of the discrete Helmholtz operator applied to this $w^{(h)}$. What motivates our primary interest toward the residual is obviously the fact that it has a physical meaning of the distributed active control sources $g^{(h)}$, see formula (2.11). However, from the numerical analysis standpoint it is known that grid convergence of the residuals is, generally speaking, not guaranteed even if the solution itself does converge. Moreover, even though the optimization formulation that we have introduced in the beginning of Section 3 is fairly conventional, in the PDEs' perspective neither the continuous generating function $w(x)$ nor its discrete counterpart $w^{(h)}$ at the optimum can be interpreted as a solution to any traditional boundary-value problem, for which the existence and regularity results are available. As such, no standard theoretical approaches to analyzing grid convergence will directly apply here, and we shall rather regard the foregoing results as experimental findings.

Let us point out that in the context of noise cancellation on the domain Ω, the issue of grid convergence of the discrete control sources $g^{(h)}$ may, in some sense, be considered as the one of secondary importance. Indeed, the output of the controls $g^{(h)}$ always eliminates the unwanted noise on Ω [more precisely, on the grid $\mathbb{N}^+$, see formula (2.10)] no matter what particular solution from the general class (2.11), (2.12) is used. Moreover, this output on $\mathbb{N}^+$ can be interpreted as a discrete generalized potential of Calderon's type, which will always converge to its continuous counterpart with the rate prescribed by the approximation order of the scheme, again, irrespective of what particular $w_n^{(h)}$, $n \in \mathbb{N}^-$, and $g_m^{(h)}$, $m \in \mathbb{M}^-$, are taken to generate the potential on every given grid, see the discussion on page 11 of this paper and references [4, 12] for detail. As such, one need not be overly concerned with the rate of convergence for the discrete optimal control sources as any of those will do the cancellation job equally well in any event. The question of grid convergence for $g^{(h)}$, however, may be of a considerable independent interest, from both the theoretical and experimental standpoint. It may certainly be worth looking into in the future, even though we expect that neither theoretical nor systematic experimental analysis will be straightforward, especially in the case of general geometries. The focus of the current paper, however, is not so much on the study of grid convergence for $g^{(h)}$, but rather on building and testing the discrete quadratic optimization algorithm and applying it to a number of cases, including those for which little is known regarding the analytic solution (see Section 3.2.2).

What we also want to emphasize in the current paper is that the L_2 optimal solutions for active controls differ very substantially from the L_1 optimal solutions obtained previously in [5]. This is, of course, natural to expect, but it is also interesting to visualize and actually observe the corresponding differences. As such, we proceed with conducting the least squares minimization for the same setup that was earlier analyzed in the sense of L_1 in our paper [5] (the L_1 results are reproduced in Figure 3.1). The grid dimensions were $L = 32$ and $J = 7$; and the wavenumber k in the Helmholtz equation (1.1) was chosen $k = 0.5$. The excitation was again produced by the point source $f^- = \delta(x - x_1)$, where $x_1 = (5, 0)$. In Figure 3.2(a) we show the magnitude of the L_2-optimal active controls on the 32×7 grid. This solution indeed differs

drastically from the L_1-optimal controls that are shown in Figure 3.1. Unlike the L_1 optimum, i.e., the layer of surface monopoles, the L_2 optimal solution tends to be distributed over the entire annular region on which the control sources are supported, obviously favoring the direction toward the noise source. We have also obtained the L_2 optimal controls for the same case but on a twice as fine grid of dimension 64×13; they are shown in Figure 3.2(b). The plots in Figures 3.2(a) and 3.2(b) look very much alike, as expected.
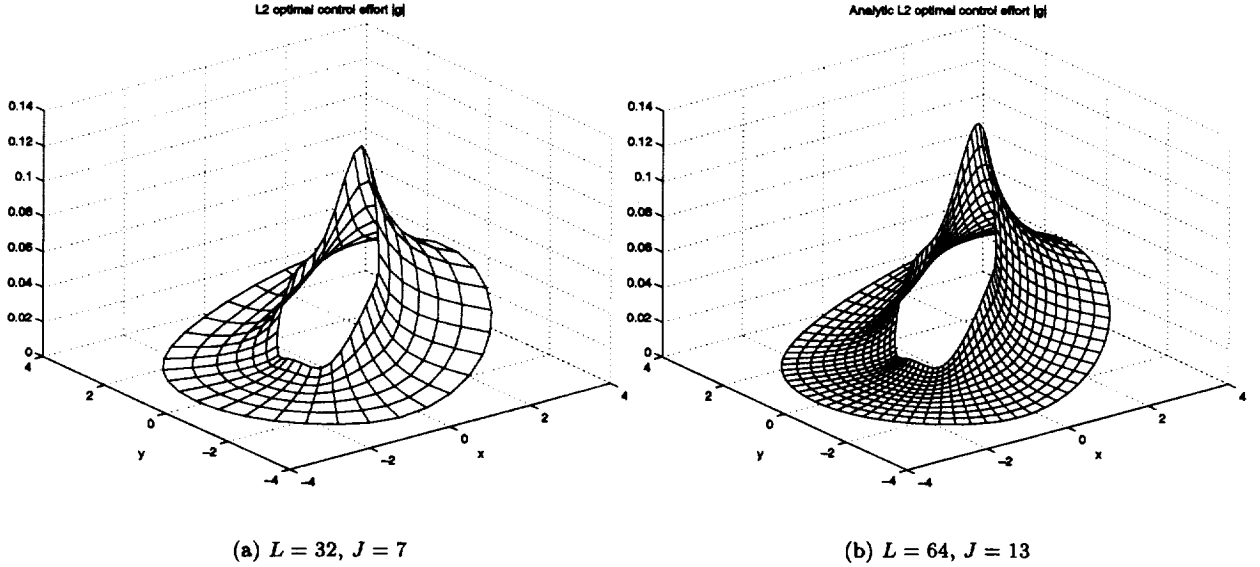

(a) $L = 32$, $J = 7$ (b) $L = 64$, $J = 13$

FIG. 3.2. *Magnitude of the L_2-optimal control sources for* $\Omega = \{x \in \mathbb{R}^2 \,||x| < 1\}$, $k = 0.5$, $f^- = \delta(x - x_1)$, $x_1 = (5, 0)$.

It is also interesting to observe how the qualitative behavior of the optimal solution changes when the parameters that define the problem change. A key parameter is the wavenumber k. Previously, we have analyzed the cases of relatively long waves compared to the size (i.e., diameter) of the protected region Ω. Let us now take $k = \pi$, then there will be exactly one full wavelength across the diameter. We compute this case on the grid 128×9 so that $1 = \rho_0 \leq \rho \leq \rho_{J-1} \approx 1.481$. In Figure 3.3, we present the distribution of optimal controls $g^{(h)}$ for the case of the long waves, $k = 0.5$ [Figure 3.3(a)], and for the case of the wavelength comparable to the domain size, $k = \pi$ [Figure 3.3(b)]. One can clearly see that the solution that corresponds to shorter waves is more oscillatory.

3.2.2. Constrained Optimization in the Sense of L_2. The purpose of formulating and solving the L_2 optimization problems that involve constraints was to simulate not simply a more sophisticated geometry but also a more realistic one. For example, if we interpret the previously considered protected region — a unit disk — as a section of the aircraft fuselage, then we can also introduce portholes, i.e., windows, that shall be interpreted as designated areas, in which no control sources can be applied. Optimization problem (3.5) in this case needs to be modified. Instead of simply finding a weak solution of $Ez = f$ in the sense of the least squares, we will now have to impose additional constraints, i.e., require that for those nodes of the grid M^- that happen to be inside the aforementioned designated areas, the corresponding equations be
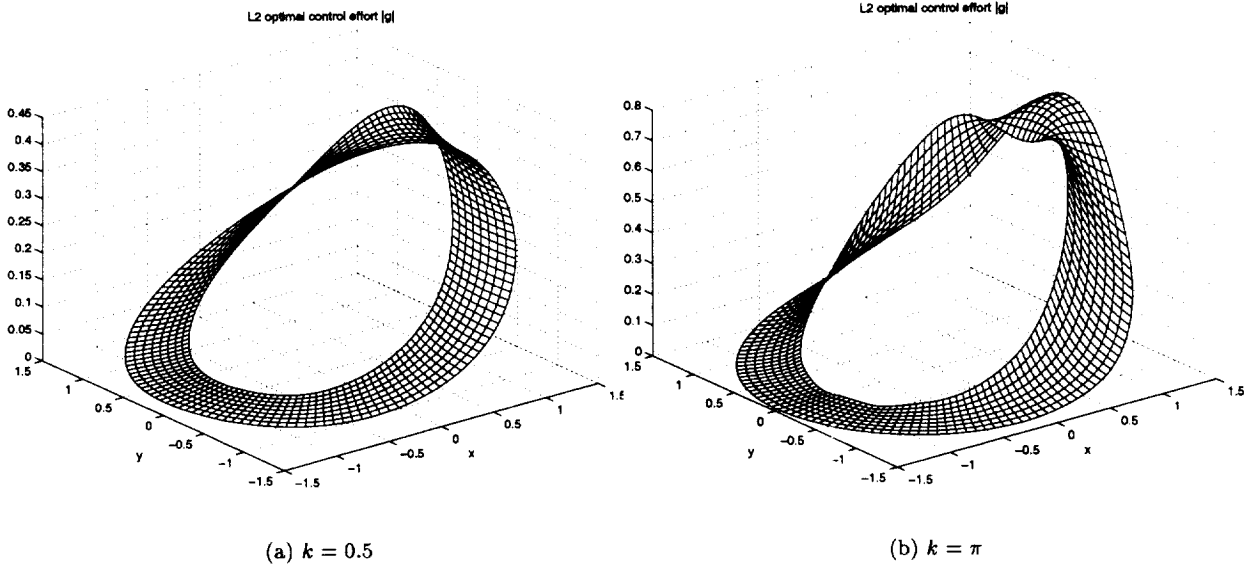
(a) $k = 0.5$ (b) $k = \pi$

FIG. 3.3. *Magnitude of the L_2-optimal control sources for $\Omega = \{x \in \mathbb{R}^2 \big| |x| < 1\}$, $f^- = \delta(x - x_1)$, $x_1 = (5,0)$, 128×9 grid.*

enforced exactly. This leads to the problem

$$\min_z \|Ez - f\|_2 \quad \text{subject to} \quad E_c z = f_c, \tag{3.12}$$

where E_c is the sub-matrix of E (i.e., the appropriate set of rows), and f_c is the respective sub-vector of f, that correspond to the constrained nodes.

For simulations, we have introduced two symmetrically located portholes in the fuselage: $5° < \theta < 30°$ and $150° < \theta < 175°$. The resulting problem (3.12) was solved by a standard methodology for the least squares minimization with equality constraints. It requires that the constraints be linearly independent and basically results in reducing the dimension of the remaining search space accordingly. In our computations, we have used the procedure LSQLIN available in MATLAB.

The case that we have actually analyzed in the context of the constrained L_2 optimization, was again one of those that we have studied previously in the L_1 framework, see [5], but obviously with no constraints. For this case, the excitation is provided by a pair of external sources: $f^- = \delta(x - x_1) + \delta(x - x_2)$, where $x_1 = (5,0)$ and $x_2 = (1,2)$, the wavenumber $k = 0.9$, and the original grid has the dimension 48×9. In Figure 3.4(a), we show the constrained L_2 optimal solution for this original grid, and in Figure 3.4(b) we show the solution for the twice as fine grid 96×17. We emphasize the presence of the large spikes in the control effort next to the boundaries of the window on the right, which is natural to expect. We should also point out at some apparent discrepancies between the control field on Figure 3.4(a) and that on Figure 3.4(b) in the region near this window. Qualitatively, these discrepancies are easily explained once we realize that a given window, which is defined as a particular range of θ, does not have to be exactly the same on different grids because of the finite size $\Delta\theta$, and a finer grid simply provides for a "sharper" definition of the window in the discrete sense. On the other hand, quantitatively we, of course, cannot claim that the same convergence results as we have obtained previously in the case with no constraints, see Section 3.2.1, will hold in the presence of the constraints as well. Moreover, in the constrained case one should generally expect less
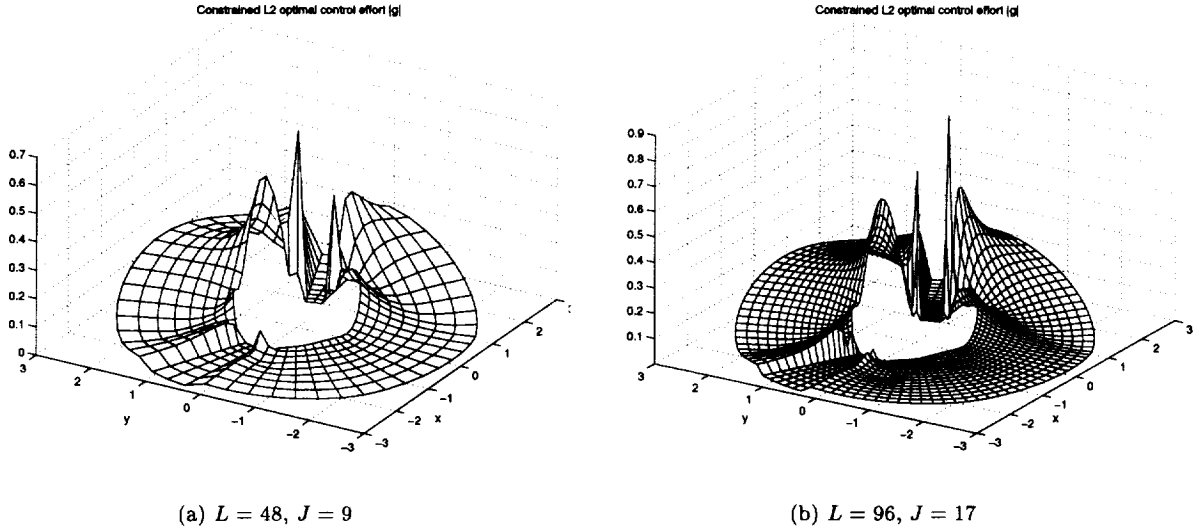
(a) $L = 48$, $J = 9$ (b) $L = 96$, $J = 17$

FIG. 3.4. *Magnitude of the L_2-optimal control sources for $\Omega = \{x \in \mathbb{R}^2 | |x| < 1\}$, $k = 0.9$, excitation: $f^- = \delta(x - x_1) + \delta(x - x_2)$, $x_1 = (5,0)$, $x_2 = (1,2)$, and window constraints: $5° < \theta < 30°$ and $150° < \theta < 175°$.*

regularity from the corresponding continuous solution than in the previously addressed unconstrained cases. Therefore, the results of the L_2 constrained minimization outlined in this Section should only be regarded as implementation examples of a previously tested numerical algorithm for more elaborate settings.

TABLE 3.3

Comparison of the computed L_2-optimal solutions with surface monopoles.

Grid	$\min\limits_{w^{(h)}} \left\| g^{(h)} \right\|_2^{(h)}$	Constrained $\min\limits_{w^{(h)}} \left\| g^{(h)} \right\|_2^{(h)}$	$\left\| g_{monopole}^{(h,surf)} \right\|_2^{(h)}$
48×9	0.41855	0.54013	1.2983
96×17	0.43485	0.56175	1.8315

It is also interesting to compare the actual norms of the solutions that we have obtained. They are presented in Table 3.3, which also contains the L_2 norms of surface monopoles that are optimal in the sense of L_1, see [5]. From Table 3.3 we see that the L_2 norm at the minimum is considerably larger for the constrained case compared to the unconstrained case. As concerns the L_2 norm of the L_1-optimum, it is three times larger in this case than the unconstrained L_2 minimum. We should also mention that the finer the grid, the larger the L_2 norm of $g_{monopole}^{(h,surf)}$ is, see Table 3.3. This is, in fact, a natural consequence of the scaling that we have adopted in [5]. Indeed, as indicated in [5], the actual magnitude of $g_{monopole}^{(h,surf)}$ increases when the grid is refined, because the corresponding continuous limit is a single layer on the interface. The latter is a singular distribution, which is obviously not integrable by itself, and even less so with square. At the same time, it turns out that the discrete two-dimensional L_1 norm of surface monopoles $\left\| g_{monopole}^{(h,surf)} \right\|_{1,M^-}$ does not change with the change of the grid size. This essentially implies that the magnitude of $g_{monopole}^{(h,surf)}$ scales as $\mathcal{O}(h^{-1})$ and as such, the L_2 norm $\left\| g_{monopole}^{(h,surf)} \right\|_{2,M^-}$ is supposed to scale as $\mathcal{O}(h^{-1/2})$. This is corroborated by the data in the last column of Table 3.3.

4. Discussion. We have developed and implemented a computational algorithm for optimizing the sources of active control of sound in the sense of L_2. For simple cases, we have been able to validate our numerical results against the analytic solution. We have also seen that the L_2 optimal controls are distinctly different from the L_1 optimal controls obtained previously. For the case of a somewhat more realistic geometry, the corresponding optimization formulation involves constraints of equality type. Our algorithm allows us to analyze the constrained L_2 optimization problems as well.

In general, we should mention that there is a multitude of different acceptable optimization criteria for active control of sound. For example, the advantage of L_1 is its clear physical interpretation as minimization of the overall absolute acoustic source strength. L_2 does not have such a transparent physical meaning, but is easier to compute numerically. In the forthcoming paper[6], we will report the results of the power optimization. It turns out that the corresponding analysis necessarily involves interaction between the sources of sound and the surrounding acoustic field, which is not the case for either L_1 or L_2. Even though it may first seem counterintuitive, one can build a control system that would require no power input for operation and would even produce a net power gain while providing the exact noise cancellation. Of course, other functions of merit, besides the aforementioned three, can be employed as well. Some may come from the engineering limitations, others will be just a matter of personal preference. Questions related to the optimization of active controls of sound using different criteria will be studied in the future.

REFERENCES

[1] S. J. ELLIOT, *Signal Processing for Active Control*, Academic Press, San Diego, 2001.

[2] C. R. FULLER, S. J. ELLIOT, AND P. A. NELSON, *Active Control of Vibration*, Academic Press, London, 1996.

[3] L. D. LANDAU AND E. M. LIFSHITZ, *Fluid Mechanics*, Pergamon Press, Oxford, 1986.

[4] J. LONČARIĆ, V. S. RYABEN'KII, AND S. V. TSYNKOV, *Active shielding and control of noise*, SIAM J. Applied Math., 62 (2001), pp. 563–596.

[5] J. LONČARIĆ AND S. V. TSYNKOV, *Optimization of acoustic source strength in the problems of active noise control*, SIAM J. Applied Math., (2003). To appear. Also: Tech. Report No. 2002–11, NASA/CR–2002–211636, ICASE, Hampton, VA, May 2002.

[6] C. L. MORFEY, *Dictionary of Acoustics*, Academic Press, San Diego, 2001.

[7] P. A. NELSON AND S. J. ELLIOT, *Active Control of Sound*, Academic Press, San Diego, 1999.

[8] Y. NESTEROV AND A. NEMIROVSKY, *Interior Point Polynomial Methods in Convex Programming: Theory and Algorithms*, SIAM Publications, Philadelphia, 1993.

[9] Y. NESTEROV AND M. J. TODD, *Self-scaled barriers and interior-point methods for convex programming*, Mathematics of Operations Research, 22 (1997), pp. 1–42.

[10] T. W. ROBERTS, D. SIDILKOVER, AND S. V. TSYNKOV, *On the combined performance of non-local artificial boundary conditions with the new generation of advanced multigrid flow solvers*, Computers and Fluids, 31 (2001), pp. 269–308.

[11] V. S. RYABEN'KII, *Necessary and sufficient conditions for good definition of boundary value problems*

---

[6]J. Lončarić and S. V. Tsynkov, *Optimization of power in the problems of active control of sound*, In progress, (2002).

for systems of ordinary difference equations, U.S.S.R. Comput. Math. and Math. Phys., 4 (1964), pp. 43–61.

[12] ———, *Method of Difference Potentials and Its Applications*, Springer-Verlag, Berlin, 2002.

[13] J. F. STURM, *Using SeDuMi 1.02, a MATLAB toolbox for optimization over symmetric cones*, Optimization Methods and Software, 11–12 (1999), pp. 625–653. Special issue on Interior Point Methods (CD supplement with software).

[14] S. V. TSYNKOV, *Numerical solution of problems on unbounded domains. A review*, Appl. Numer. Math., 27 (1998), pp. 465–532.

[15] ———, *On the definition of surface potentials for finite-difference operators*, J. Sci. Comput., 18 (2003), pp. 155–189. To appear. Also: Tech. Report No. 2001-23, NASA/CR–2001–211059, ICASE, Hampton, VA, August 2001.

[16] R. J. VANDERBEI, *Linear Programming: Foundations and Extensions*, Kluwer Academic Publishers, Boston, 2001.

[17] R. I. VEIZMAN AND V. S. RYABEN'KII, *Difference problems of screening and simulation*, Dokl. Akad. Nauk, 354 (1997), pp. 151–154.

[18] ———, *Difference simulation problems*, in Transactions of Moscow Mathematics Society, 1997, pp. 239–248.

[19] Y. YE, M. J. TODD, AND S. MIZUNO, *An $O(\sqrt{n}L)$-iteration homogeneous and self-dual linear programming algorithm*, Mathematics of Operations Research, 19 (1994), pp. 53–67.

REPORT DOCUMENTATION PAGE

1. AGENCY USE ONLY*(Leave blank)*	2. REPORT DATE October 2002	3. REPORT TYPE AND DATES COVERED Contractor Report	

4. TITLE AND SUBTITLE
QUADRATIC OPTIMIZATION IN THE PROBLEMS OF ACTIVE CONTROL OF SOUND

5. FUNDING NUMBERS
C NAS1-97046
WU 505-90-52-01

6. AUTHOR(S)
J. Loncaric and S.V. Tsynkov

7. PERFORMING ORGANIZATION NAME(S) AND ADDRESS(ES)
ICASE
Mail Stop 132C
NASA Langley Research Center
Hampton, VA 23681-2199

8. PERFORMING ORGANIZATION REPORT NUMBER
ICASE Report No. 2002-35

9. SPONSORING/MONITORING AGENCY NAME(S) AND ADDRESS(ES)
National Aeronautics and Space Administration
Langley Research Center
Hampton, VA 23681-2199

10. SPONSORING/MONITORING AGENCY REPORT NUMBER
NASA/CR-2002-211939
ICASE Report No. 2002-35

11. SUPPLEMENTARY NOTES
Langley Technical Monitor: Dennis M. Bushnell
Final Report
To be submitted to the SIAM Journal on Applied Mathematics.

12a. DISTRIBUTION/AVAILABILITY STATEMENT

Unclassified–Unlimited
Subject Category 64
Distribution: Nonstandard
Availability: NASA-CASI (301) 621-0390

12b. DISTRIBUTION CODE

13. ABSTRACT *(Maximum 200 words)*
We analyze the problem of suppressing the unwanted component of a time-harmonic acoustic field (noise) on a predetermined region of interest. The suppression is rendered by active means, i.e., by introducing the additional acoustic sources called controls that generate the appropriate anti-sound. Previously, we have obtained general solutions for active controls in both continuous and discrete formulations of the problem. We have also obtained optimal solutions that minimize the overall absolute acoustic source strength of active control sources. These optimal solutions happen to be particular layers of monopoles on the perimeter of the protected region. Mathematically, minimization of acoustic source strength is equivalent to minimization in the sense of L_1.

By contrast, in the current paper we formulate and study optimization problems that involve quadratic functions of merit. Specifically, we minimize the L_2 norm of the control sources, and we consider both the unconstrained and constrained minimization. The unconstrained L_2 minimization is certainly the easiest problem to address numerically. On the other hand, the constrained approach allows one to analyze sophisticated geometries. In a special case, we can compare our finite-difference optimal solutions to the continuous optimal solutions obtained previously using a semi-analytic technique. We also show that the optima obtained in the sense of L_2 differ drastically from those obtained in the sense of L_1.

14. SUBJECT TERMS
noise cancellation, active control sources, volumetric and surface controls, general solution, monopoles and dipoles, radiation of waves, complex-valued quantities, L_2 minimization, overdetermined systems, least squares, unconstrained minimization

15. NUMBER OF PAGES
29

16. PRICE CODE
A03

17. SECURITY CLASSIFICATION OF REPORT Unclassified	18. SECURITY CLASSIFICATION OF THIS PAGE Unclassified	19. SECURITY CLASSIFICATION OF ABSTRACT	20. LIMITATION OF ABSTRACT